Journal of the Korean Ceramic Society (2020) 57:570–577
https://doi.org/10.1007/s43207-020-00051-y

ORIGINAL ARTICLE

Effect of $SrTiO_3$ modification on dielectric, phase transition and piezoelectric properties of lead-free $Bi_{0.5}Na_{0.5}TiO_3$−$CaTiO_3$−$SrTiO_3$ piezoelectric ceramics

Hoang Thien Khoi Nguyen[1] · Trang An Duong[1] · Farrukh Erkinov[1] · Hyungwon Kang[2] · Byeong Woo Kim[3] · Chang Won Ahn[4] · Hyoung-Su Han[1] · Jae-Shin Lee[1]

Received: 6 February 2020 / Revised: 16 April 2020 / Accepted: 17 April 2020 / Published online: 7 May 2020

Abstract
This study investigated the structures, dielectric, ferroelectric and piezoeletric properties of lead-free $(0.99-x)Bi_{0.5}Na_{0.5}TiO_3$−$0.01CaTiO_3$−$xSrTiO_3$ (BNT−CT−100xST, $x = 0.22$–0.30) piezoelectric ceramics. These piezoceramics were successfully prepared using the conventional solid-state reaction method sintered at 1175 °C for 2 h. It was found that a phase transition from nonergodic relaxor to ergodic relaxor was induced by ST modification in BNT−CT ceramics. Consequently, a large electromechanical strain of 0.20% corresponding to high normalized strain d^*_{33} of 667 pm/V was obtained even under 3 kV/mm for BNT−CT−28ST ceramics. Therefore, it is noted that lead-free BNT−CT−100xST ceramics can be promising candidates for actuator applications.

Keywords Piezoelectric properties · Dielectric properties · Lead-free · Relaxor · Ternary system

1 Introduction

Piezoelectric materials have attracted a great deal of attention for electronic devices, such as actuators, transducers and sensors, etc. The most widely used piezoelectric material are $PbTiO_3$−$PbZrO_3$ (PZT)-based component systems [1]. However, volatilization of toxic PbO during high temperature sintering not only causes environmental pollution, but also generates instability of composition and electrical properties of the final products. It is recently desired to use lead-free materials for environmental protection; and in many countries (European Union, Japan, Korea, etc.), the governments have encouraged the industry to remove lead from electric and electronic equipment [2–5]. Accordingly, lead-free piezoelectric materials concerned with ceramics based on $(K_{0.5}Na_{0.5})NbO_3$ (KNN) and $Bi_{1/2}Na_{1/2}TiO_3$ (BNT) have been widely attracting attention to replace PZT ceramics [6–10].

Especially, Bi-based lead-free piezoceramics such as $Bi_{1/2}Na_{1/2}TiO_3$−$BaTiO_3$ (BNT−BT) or $Bi_{1/2}Na_{1/2}TiO_3$−$Bi_{1/2}K_{1/2}TiO_3$ (BNKT) materials have been considered as potential candidates for actuator applications because of their excellent electromechanical strain properties. Those bismuth-based materials possess a reversible phase transition between an ergodic ralaxor state and a ferroelectric with the application of electric field that results in an abnormal electromechanical strain [11–16]. However, the required electric field to obtain large strain is twice as high as the field used to achieve maximum polarization and strain in typical soft PZT system, which is one of the critical problems for use in practical applications [15].

One material to overcome this problem is BNT−$SrTiO_3$ (BNT−ST) ceramics. This system was firstly reported by Sakata and Masuda [17]. It revealed that phase transition in BNT−ST system with respect to room temperature from rhombohedral to pseudo-cubic phase occurs around 20–25 mol% ST [18], accompanying with a considerable

✉ Hyoung-Su Han
hsejs@ulsan.ac.kr

[1] School of Materials Science and Engineering, University of Ulsan, Ulsan, Republic of Korea

[2] Electronic Convergence Materials and Device Research Center, Korea Electronic Technology Institute, Seongnam-si, Republic of Korea

[3] Department of Electrical Engineering, University of Ulsan, Ulsan, Republic of Korea

[4] Department of Physics and EHSRC, University of Ulsan, Ulsan, Republic of Korea

effect on the electromechanical properties. The maximum piezoelectric constant (d_{33}) value of 127 pC/N at around 24 mol% ST, followed by decreasing markedly d_{33} value to no piezoelectric response with more than 28 mol% ST, at which it exhibits a large strain reaching values of 0.29% at 6 kV/mm. This high strain is attributed to the reversible electric-field-induced phase transition between relaxor and ferroelectric phase [19]. Furthermore, many researchers are recently investigating BNT−ST ceramics with amount of ST around 25–26 mol% showed a very high strain ~ 0.26% at electric field as low as 4 kV/mm [20–24].

Besides, the effect of other alkaline-earth metal ion doping, such as Ca^{2+}, on the electrical properties and phase transition behaviors of BNT ceramics were conducted by Watanabe et al. [25]. According to this study, Ca^{2+} substitution led to a decrease of the depolarization temperature (T_d) which seems to relate to the reduction of rhombohedral distortion in Ca-substituted BNT ceramics [25]. It was found that the rate of T_d dropped down to room temperature in the Ca-substituted BNT system was faster than that in the Sr substitution, therefore, maximum values of piezoelectric properties could be obtained at a very small amount ~ 2 at% of Ca^{2+} substitution [25].

Recently, many studies have further improved the actuating performance by forming BNT-based ternary phase systems such as $Bi_{0.5}Na_{0.5}TiO_3$−$KNbO_3$−$SrTiO_3$ [26], $Bi_{0.5}Na_{0.5}TiO_3$−$BaTiO_3$−Sr_2MnSbO_6 [27], $Bi_{0.5}Na_{0.5}TiO_3$−$SrTiO_3$−$LiNbO_3$ [28], $Bi_{0.5}Na_{0.5}TiO_3$−$BaTiO_3$−$Bi(Mn_{0.5}Ti_{0.5})O_3$ [29] and so on. On the other hand, few researches have been studied on piezoelectric properties and phase transition behavior of BNT−$CaTiO_3$-based system [30, 31].

From these background, we tried to synthesize (0.99−x) $Bi_{0.5}Na_{0.5}TiO_3$−0.01$CaTiO_3$−$x$$SrTiO_3$ (BNT−CT−100xST) ceramics as a new BNT-based ternary system. This study systemically investigated the structures, dielectric and ferroelectric properties of BNT−CT−100xST ceramics.

2 Experimental procedure

BNT-based lead-free piezoceramics with the compositions of BNT−CT−100xST (x = 0.22, 0.24, 0.26, 0.28 and 0.30) ceramics were prepared by a conventional solid-state reaction method. The component oxide and carbonate powders, Bi_2O_3 (99.9%), TiO_2 (99.0%), Na_2CO_3 (99.8%), $CaCO_3$ and $SrCO_3$ (99.0%), were used as raw materials (High Purity Chemicals, Japan). The raw materials were mixed in stoichiometric proportions by conventional ball milling treatment in ethanol using ZrO_2 balls, then dried and calcined at 850 °C for 2 h to form the uniform solid solution. The resultant powders were mixed with the polyvinyl alcohol (PVA) binder and then pressed into green discs with a diameter of 12 mm under a uniaxial pressure of 98 MPa. Finally, the pellets were placed in a sealed alumina crucible that was thermally treated to remove PVA at 550 °C for 30 min then sintered at 1175 °C for 2 h.

The density of the sintered ceramics was measured using Archimedes' immersion principle method using a digital densiometer (SD-120L, A&D, Japan). To determine relative density value, the theoretical density of each compositions was calculated using the formula:

$$\rho = \frac{\sum A_C + \sum A_A}{V_C \times N_A}, \quad (1)$$

where $\sum A_C$: the sum of the atomic weights of all cations in the formula unit. $\sum A_A$: the sum of the atomic weights of all anions in the formula unit. V_C: the unit cell volume, N_A: Avogadro's number.

The crystal structure was characterized with an X-ray diffractometer (XRD, RAD III, Rigaku, Japan) using monochromatic CuKα radiation with the wavelength λ = 1.54178 Å. The polished and thermally etched surfaces of samples were imaged via Field-Emission Scanning Electron Microscopy (FE-SEM, JEOL JSM−65OFF, USA) and the crystal structure was characterized with an X-ray diffractometer (XRD, RAD III, Rigaku, Japan). For electrical measurements, a silver paste was screen printed on both sides of specimens and subsequently burnt in at 700 °C for 30 min. The polarization (P) and strain (S) hysteresis as a function of the external electric field (E) were measured with a piezoelectric measurement system (aixACCT aixPES, Aachen, Germany). The temperature-dependent dielectric constant (ε_r) and dielectric loss (tan δ) of the BNT–CT–100xST ceramics were carried out at a heating rate of 5 °C/min in a temperature-regulated chamber connected to a precision LCR meter (E4980AL, Keysight, USA) at 1, 10, and 100 kHz.

3 Results and discussion

The linear shrinkage and relative density values of BNT–CT–100xST ceramics as a function of ST content are displayed in Fig. 1. All samples exhibited around 15% values of linear shrinkage and high relative densities reached over 97%. These results indicate that the sintering temperature at 1175 °C is suitable for densification of BNT–CT–100xST ceramics regardless of ST modification.

FE-SEM images of BNT–CT–100xST ceramics display in Fig. 2. All images revealed dense microstructures, which are consistent with behaviors of relative densities for BNT–CT–100xST ceramics as can be seen in Fig. 1. The average grain size values were decreased with increasing ST content that were determined by the linear intercept method.

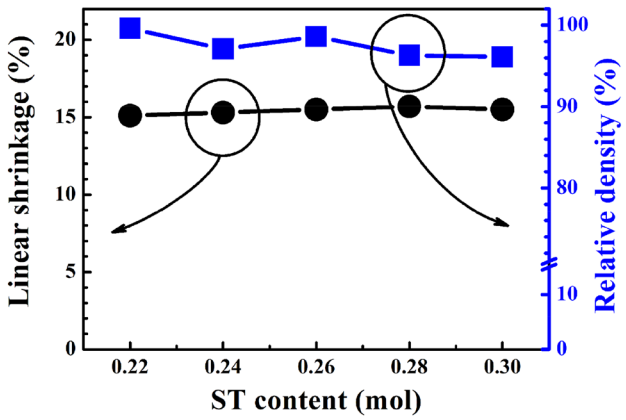

Fig. 1 Linear shrinkage and relative density values of BNT–CT–100*x*ST ceramics as a function of ST content

The largest AGS was 9.42 ± 1.19 μm for BNT–CT–22ST ceramics and the smallest AGS was 5.48 ± 0.62 μm for the BNT–CT–30ST ceramics. The changes are consistent with previous results in the microstructures of ST-modified BNT-based ceramics [24, 32], which seems to be closely related to the thermodynamic behaviors of the synthesized materials and diffusion behavior of Sr [33, 34]. It was reported that the temperatures required for the formations of BNT and ST phases start at around 530 °C and 560 °C, respectively [35, 36]. In detail, at 530 °C BNT phase is formed due to the decomposition of Na_2CO_3 and its reaction with Bi_2O_3 and TiO_2. The densification of BNT phase structure goes on with subsequent Sr^{2+} diffusion from decomposing $SrCO_3$ [33]. It is noticed that the transport of Sr^{2+} occurs along grain boundaries rather than through the BNT phase [34]. The development of ST mainly at grain boundary results in the formation of core–shell structure [33, 34]. Accordingly, this phenomenon might be responsible for the suppressed grain growth in BNT–ST systems. Therefore, the different reaction temperatures of two materials are suggested to be the origin of the decreased grain size with increasing the ST doping level.

Figure 3 presents XRD patterns of BNT–CT–100*x*ST ceramics at room temperature. In Fig. 3, all samples exhibited single perovskite phases, demonstrating that a uniform solid solution was formed. From Fig. 3b, c, the BNT–CT–100*x*ST ceramics showed a single cubic perovskite structure as evidence by no peak splitting in ranges of 39.7°−40.3° and 45.9°−47.1° except for $K\alpha_2$ peaks. This feature is normally observed in BNT-based relaxor materials [37, 38]. Accordingly, it may assume that all compositions in this study can be categorized as the relaxor materials. Besides, the lattice parameters were increased with increasing the ST content as evidenced by shifting to lower angle of (111) and (002) peaks. The reason for this change is that the ionic radius of Sr^{2+} (1.32 Å) is bigger than the averaged A-site ionic radius of BNT–CT (Bi^{3+}: 1.17 Å, Na^{1+}: 1.16 Å and Ca^{2+}: 1.00 Å) [25]. This result implies that the modified ST does not affect the crystal structure change in BNT–CT system, which is well matched with other BNT-based lead-free relaxor materials [39–43].

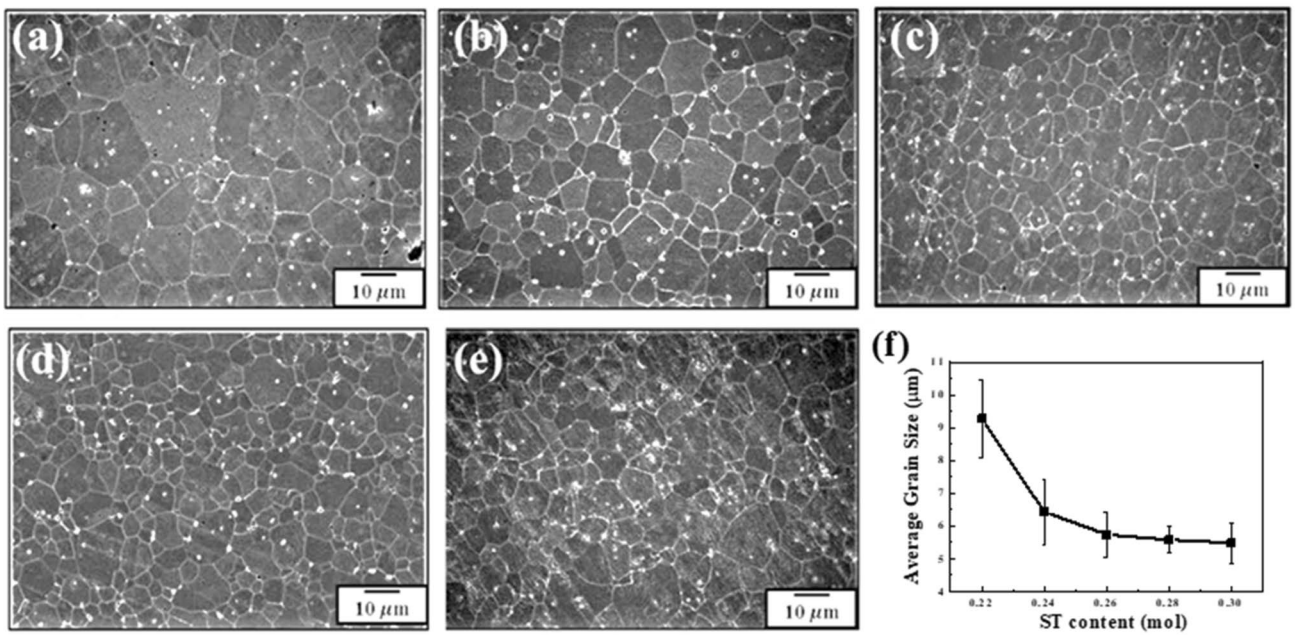

Fig. 2 FE-SEM images of polished and thermally etched BNT–CT–100*x*ST ceramics, **a** $x = 0.22$, **b** $x = 0.24$, **c** $x = 0.26$, **d** $x = 0.28$, **e** $x = 0.30$ and **f** the average grain size as a function of ST content

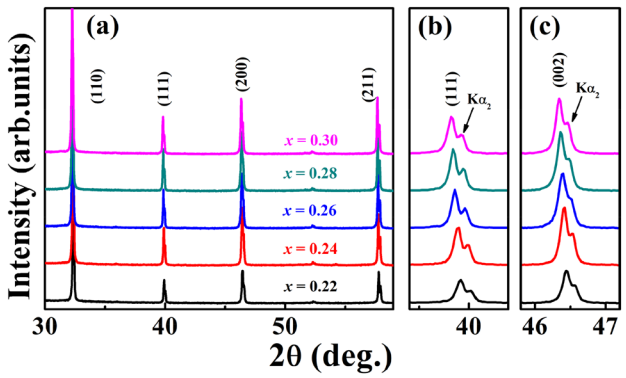

Fig. 3 X-ray diffraction patterns of BNT–CT–100*x*ST ceramics as a function of ST content, **a** 20−60°, **b** 39.5−41.5°, and **c** 46.5−47.5°

Figure 4 shows the temperature dependence of dielectric constant (ε_r) and dielectric loss (tan δ) for both unpoled and poled BNT–CT–100*x*ST ceramics with three measurement frequencies of 1, 10 and 100 kHz. All the poled and unpoled specimens showed a strong frequency dispersion and broadened peaks in dielectric spectra, implying that BNT–CT–100*x*ST ceramics can be categorized as relaxors. Furthermore, poled BNT–CT–22ST ceramics revealed two abnormal peaks. The first one is referred to as T_m, which denotes the temperature giving the maximum dielectric constant. As shown in Fig. 4, with increasing ST content, T_m shifted toward lower temperatures from 230 °C for BNT–CT–22ST ceramics to 142 °C for BNT–CT–30ST ceramics which is consistent with observations reported in previous studies [19, 24, 32, 44]. The second anomaly peak located at the lower temperature region corresponds to T_{F-R} (the ferroelectric-to-relaxor transition temperature), where the electric-field-induced long-range order breaks down into a short-range one [38, 45]. This result shows that BNT–CT–22ST ceramics is a nonergodic relaxor (NER) at low temperature. We should note that the determination of T_{F-R} is only valid for poled specimens [14, 37, 39, 40]. It is also seen that T_{F-R} decreased from ~ 40 °C for BNT–CT–22ST ceramics to ~ 30 °C for BNT−CT−24ST

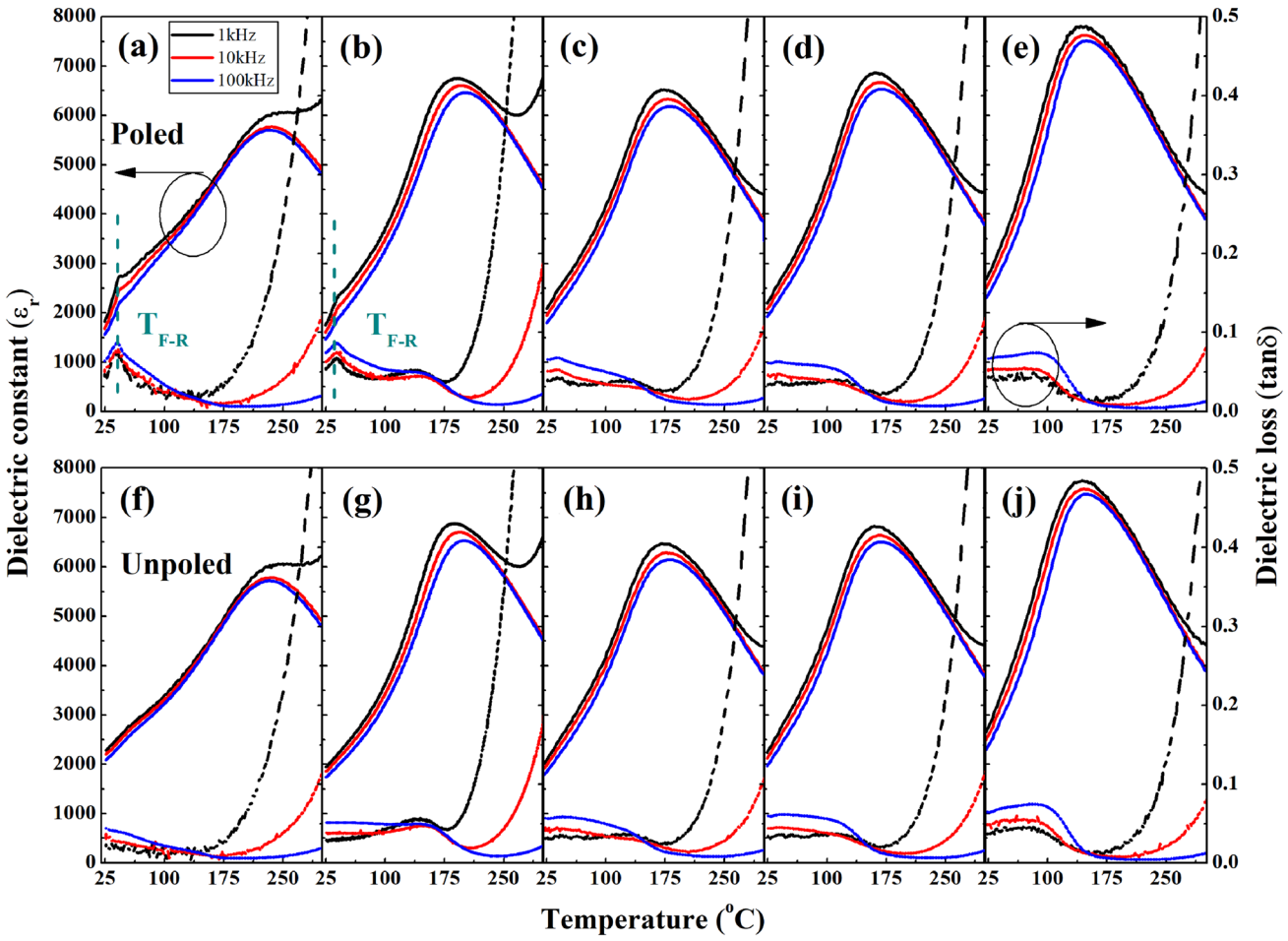

Fig. 4 Temperature-dependent dielectric constant (ε_r) and dielectric loss (tan δ) for the poled (top) and unpoled (bottom) BNT–CT–100*x*ST ceramics as a function of ST content, **a** and **f** $x = 0.22$, **b** and **g** $x = 0.24$, **c** and **h** $x = 0.26$, **d** and **i** $x = 0.28$, **e** and **j** $x = 0.30$

ceramics and then was not detectable for the compositions with higher ST contents. The absence of apparent T_{F-R} for poled BNT−CT−100xST ceramics with $x \geq 0.26$ in the range measurement data was an indication that lowering of T_{F-R} below the room temperature. This implies that those specimens were ergodic relaxors (ER), in which the field-induced changes were recovered back to their initial state on removal of the electric field at the room temperature [46].

The polarization (P−E) and bipolar strain (S−E) curves of BNT−CT−100xST at the applied electric fields of 4 kV/mm are depicted in Fig. 5. Typical ferroelectric hysteresis curves, represented by square-type polarization and butterfly-shaped strain hysteresis, were observed for BNT−CT−22ST and BNT−CT−24ST ceramics. As discussed above in reference to Fig. 4, those two compositions are NER at room temperature with microscopic cubic structures at zero electric field. When an electric field is applied to the NER materials, it can transform irreversibly into a ferroelectric state [47–49]. Therefore, we can observe the square-shaped P−E curves with butterfly-shaped strain curves of BNT−CT−22ST and BNT−CT−24ST ceramics. A further increase in ST modification led to drastic decreases in remanent polarizations (P_r), coercive fields (E_C) with double hysteresis P−E curves and large strains. The changes in polarization and strain curves such as the drastically decreased E_c, P_r, negative strain (S_{neg}), and increased maximum strain (S_{max}) for $x = 0.28$ ceramics can be categorized an incipient piezoceramics as ER [15]. Those large strains are observed in other BNT-based relaxor materials, which are originated from the reversible transition into a ferroelectric state [39–43].

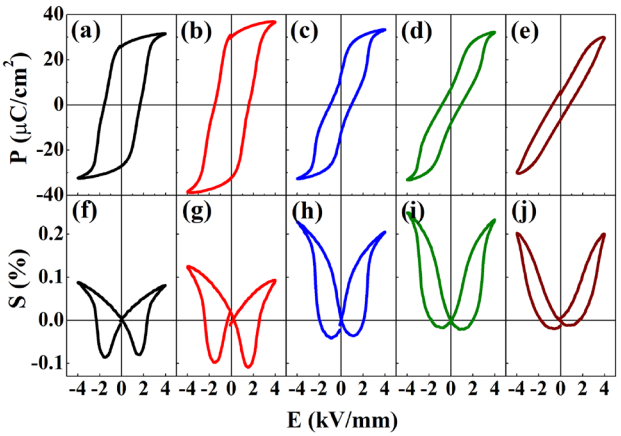

Fig. 5 Polarization (top) and bipolar strain curves (bottom) for BNT−CT−100xST ceramics as a function of ST content, **a** and **f** $x = 0.22$, **b** and **g** $x = 0.24$, **c** and **h** $x = 0.26$, **d** and **i** $x = 0.28$, **e** and **j** $x = 0.30$

For better understanding effects of ST modification, characteristic parameters such as E_c, P_r, maximum polarization (P_{max}), S_{max}, and S_{neg} were extracted from Fig. 5 and are plotted in Fig. 6. The ferroelectric BNT−CT−24ST ceramics showed good P_r and E_c around 30.9 μC/cm^2 and 1.56 kV/mm, respectively. However, when the ST content increased those values decreased drastically with strongly pinched P−E curves. Therefore, P_r and E_c reached minimum values as 5.32 μC/cm^2 and 0.68 kV/mm when the modification level of ST was 30 mol%. On the other hand, P_{max} values for BNT−CT−100xST ceramics were changed slightly with increasing ST modification. These results in P−E curves imply that FE−to−RE phase transition in BNT−CT−100xST ceramics was induced by ST modification. The values of S_{max} increased with increasing x from 0.22 to 0.28, and then decreased with further increases in ST content. BNT−CT−28ST ceramics showed the highest S_{max} under the applied electric field of 4 kV/mm of 0.25%.

The unipolar strain curves are plotted in Fig. 7 with applying electric field as 3 and 4 kV/mm. BNT−CT−22ST and BNT−CT−24ST ceramics exhibited linear unipolar strain curves which are categorized as stabilized FE compositions. On the other hand, with further increases in the ST content, the strain value increased drastically with getting larger hysteresis for $0.24 < x < 0.30$, and then was declined in BNT−CT−30ST ceramics. We obtained the largest strain properties in BNT−CT−28ST ceramics regardless

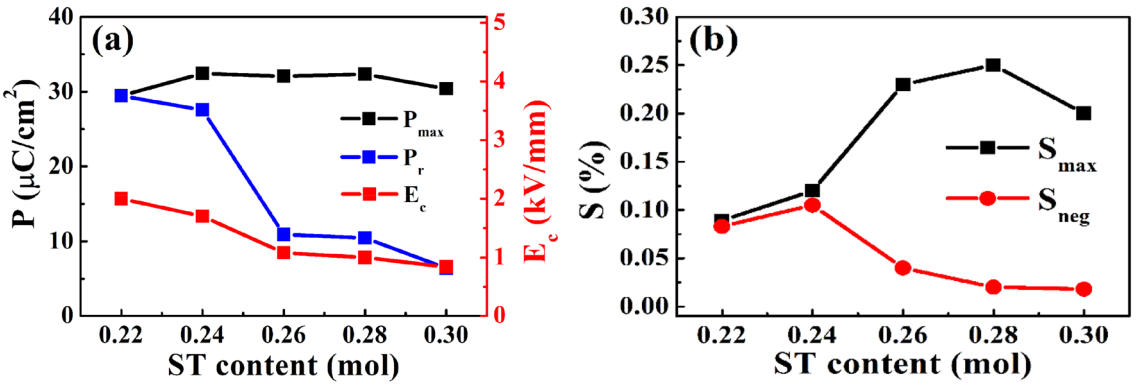

Fig. 6 Variation of **a** E_c, P_r, and **b** S_{max}, S_{neg} of BNT−CT−100xST ceramics as a function of ST content

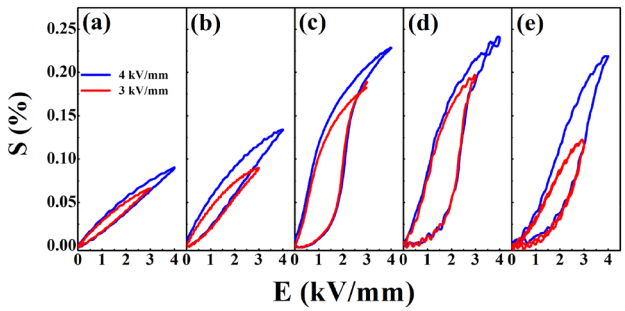

Fig. 7 Unipolar strain curves for BNT−CT−100*x*ST ceramics as a function of ST content

of applied electric fields, which gave the maximum strain of 0.20% and 0.24% under 3 and 4 kV/mm, respectively. This large unipolar strain is attributed to the ferroelectric-to-relaxor phase transition induced by ST modification that was originated from the interrupted long-range ferroelectric order [38, 45].

To confirm the achievement of this study, the characteristic parameters such as the S_{max}, applied electric field (E_{max}), and the normalized strain (d^*_{33}) were extracted and calculated from Fig. 7, which were compared with other piezoceramics in Table 1. From previous studies, many high d^*_{33} values of lead-free ceramics had been reported for BNT−BKT−ST5 (600 pm/V) [38], Nb-doped BNKT (641 pm/V) [50], and BNT−BT−KNN2 (560 pm/V) [51]. However, those ceramics required relatively strong electric fields (around 6–8 kV/mm as E_{max}) to obtain large strains, which is a drawback for practical applications mentioned above. In our work, a decrease of the driving field from 6 to 3 kV/mm could be obtained for BNT−CT−26ST and BNT−CT−28ST. Furthermore, by utilizing the BNT−CT−ST ternary ceramics, the field-induced-strain behaviors have been improved upon BNT−ST binary materials. For detailed, BNT−CT−28ST ceramics showed the large d^*_{33} value of 667 pm/V, which is higher than 625 pm/V of BNT−28ST [24]. The main reason for the relatively enhanced strain of this system is unclear yet. However, it found that some difference between polarization and strain curves in BNT−CT−ST ceramics as this study and in BNT−28ST ceramics. There were two facts that one was obtained a relatively broader polarization hysteresis and the other was observed a relatively deeper and larger S_{neg} in comparison to BNT−28ST ceramics. From these results, we may assume that the induced nonergodicities by added CT are responsible for relatively enhancing strain properties of BNT−CT−ST ceramics in comparison to BNT−28ST ceramics [28, 37]. To clarify this assumption, it is obviously needed further study. This method could be compared with the relaxor/ferroelectric composite approaches which are recently considered as good techniques for obtaining high low-field-induced strain properties [52–54]. Therefore, we believe that BNT−CT−100*x*ST ceramics are promising candidates for actuator applications.

4 Conclusions

The effect of a ST modifier on the crystal structure and electromechanical properties of $(0.99-x)Bi_{0.5}Na_{0.5}TiO_3-0.01CaTiO_3-xSrTiO_3$ ceramics was investigated. The results showed that as the ST content was increased, a phase transition from NER to ER occurred in the system. The addition of ST shifted the T_{F-R} to a lower temperature and destabilized the ferroelectric order resulted in the degradation of remnant polarization, coercive field, and negative strain, which was accompanied by a large electric-field-induced strain of 0.20% and a high normalized strain of d^*_{33} = 667 pm/V under a low applied electric field of 3 kV/mm for BNT−CT−28ST ceramics. These results indicated that BNT−CT−100*x*ST can be a promising candidate for actuator application.

Table 1 Comparison of normalized strains d^*_{33} (S_{max}/E_{max}) between this study and other BNT-based lead-free piezoceramics

Material	S_{max} (%)	E_{max} (kV/mm)	d^*_{33} (pm/V)	References
BNT−CT−26ST	0.185	3	617	This work
BNT−CT−28ST	0.20	3	667	This work
25ST	0.24	4	600	[20]
BNT−28ST	0.25	4	625	[24]
BNST28	0.29	6	488	[19]
BNT−BKT−ST5	0.36	6	600	[38]
Nb-doped BNKT	0.45	7	641	[50]
BNT−BT−KNN2	0.45	8	560	[51]
0.93BNKT−0.07BA/BNT	0.29	4	725	[52]
2LF/1.5SN	0.298	4	745	[53]
BNKT−0.04BMT/1.5BNT	0.14	2.5	560	[54]

Acknowledgements This study was supported by the National Research Foundation (NRF) Grant (2016R1D1A3B01008169). HS Han acknowledges financial support from the National Research Foundation (NRF) of Republic of Korea Grant (2016R1C1B1014365). CW Ahn acknowledges financial support from Basic Science Program through the National Research Foundation (NRF) of Republic of Korea funded by the Ministry of Science and ICT Grant (2018R1A2B6009210).

References

1. B. Jaffe, W. Cook, *Piezoelectric ceramics* (Academic Press, New York, 1971)
2. C.H. Hong, H.P. Kim, B.Y. Choi, H.S. Han, J.S. Son, C.W. Ahn, W. Jo, Lead-free piezoceramics—where to move on? J. Materiomics **2**, 1–24 (2016)
3. J. Rödel, K.G. Webber, R. Dittmer, W. Jo, M. Kimura, D. Damjanovic, Transferring lead-free piezoelectric ceramics into application. J. Eur. Ceram. Soc. **35**, 1659–1681 (2015)
4. A.J. Bell, O. Deubzer, Lead-free piezoelectrics-The environmental and regulatory issues. MRS Bull. **43**, 581–587 (2018)
5. J. Rödel, J.F. Li, Lead-free piezoceramics: status and perspectives. MRS Bull. **43**, 576–580 (2018)
6. J.K. Kang, J.S. Lee, Preparation of $Bi_{0.5}Na_{0.5}TiO_3$-based multilayer ceramic actuators using microwave sintering. J. Korean Inst. Electr. Electron. Mater. Eng. **27**, 702–706 (2014)
7. S. Cho, J.H. Yoo, Y.H. Jeong, Dielectric and piezoelectric properties of 0.97 $(Na_{0.52}K_{0.443}Li_{0.037})(Nb_{0.96-x}Sb_{0.04}Ta_x)O_3$–$0.03(Bi_{0.5}Na_{0.5})_{0.9}(Sr)_{0.1}ZrO_3$ ceramics for pizoelectric actuator. Trans. Electr. Electron. Mater. **20**, 328–333 (2019)
8. G. Liu, W. Jiang, K. Liu, X. Liu, C. Song, Y. Yan, L. Jin, An investigation of dielectric, piezoelectric properties and microstructures of $Bi_{0.5}Na_{0.5}TiO_3$-$BaTiO_3$-$Bi_{0.5}K_{0.5}TiO_3$ lead-free piezoelectric ceramics doped with K_2AlNbO_5 compound. J. Electron. Mater. **46**, 5287–5295 (2017)
9. Y.H. Kwon, D.J. Shin, J.H. Koh, $(1–x)(Bi, Na)TiO_{3-x}(Ba, Sr)T_iO_3$ Lead-free piezoelectric ceramics for piezoelectric energy harvesting. J. Korean Phys. Soc. **66**, 1067–1071 (2015)
10. B. Malic, J. Koruza, J. Hrescak, J. Bernard, K. Wang, J.G. Fisher, A. Bencan, Sintering of lead-free piezoelectric sodium potassium niobate ceramics. Materials **8**, 8117–8146 (2015)
11. J.K. Kang, T.H. Dinh, C.H. Lee, H.S. Han, J.S. Lee, V.D.N. Tran, Comparative study of conventional and microwave sintering of large strain Bi-based perovskite ceramics. Trans. Electr. Electron. Mater. **18**, 19–24 (2017)
12. S.T. Zhang, A.B. Kounga, E. Aulbach, H. Ehrenberg, J. Rödel, Giant strain in lead-free piezoceramics $Bi_{0.5}Na_{0.5}TiO_3$–$BaTiO_3$–$K_{0.5}Na_{0.5}NbO_3$ system. Appl. Phys. Lett. **91**, 112906–112901 (2007)
13. H.S. Han, I.K. Hong, Y.M. Kong, J.S. Lee, W. Jo, Effect of Nb doping on the dielectric and strain properties of lead-free $0.94(Bi_{1/2}Na_{1/2})TiO_3$-$0.06BaTiO_3$ ceramics. J. Korean. Ceram. Soc. **53**, 145–149 (2016)
14. T.H. Dinh, H.S. Han, J.S. Lee, C.W. Ahn, I.W. Kim, M.R. Bafandeh, Ergodicity and nonergodicity in La-doped $Bi_{1/2}(Na_{0.82}K_{0.18})_{1/2}TiO_3$ relaxors. J. Korean Phys. Soc. **66**, 1077–1081 (2015)
15. W. Jo, R. Dittmer, M. Acosta, J. Zang, C. Groh, E. Sapper, K. Wang, J. Rödel, Giant electric-field-induced strains in lead-free ceramics for actuator applications-status and perspective. J. Electroceram. **29**, 71–93 (2012)
16. A.R. Paterson, H. Nagata, X. Tan, J.E. Daniels, M. Hinterstein, R. Ranjan, P.B. Groszewicz, W. Jo, J.L. Jones, Relaxor-ferroelectric transitions: Sodium bismuth titanate derivatives. MRS Bull. **43**, 600–606 (2018)
17. K. Sakata, Y. Masuda, Ferroelectric and antiferroelectric properties of $(Na_{0.5}Bi_{0.5})TiO_3$–$SrTiO_3$ solid solution ceramics. Ferroelectrics **7**, 347–349 (1974)
18. D. Rout, K.S. Moon, S.J.L. Kang, I. Kim, Dielectric and raman scattering studies of phase transitions in the $(100–x)$ $Na_{0.5}Bi_{0.5}TiO_{3-x}SrTiO_3$ system. J. Appl. Phys **108**, 084102 (2010)
19. Y. Hiruma, Y. Imai, Y. Watanabe, H. Nagata, T. Takenaka, Large electrostrain near the phase transition temperature of $(Bi_{0.5}Na_{0.5})$ TiO_3–$SrTiO_3$ ferroelectric ceramics. Appl. Phys. Lett. **92**, 2904 (2008)
20. M. Acosta, W. Jo, J. Rödel, Temperature-and frequency-dependent properties of the $0.75Bi_{1/2}Na_{1/2}TiO_3$–$0.25SrTiO_3$ lead-free incipient piezoceramic. J. Am. Ceram. Soc. **97**, 1937–1943 (2014)
21. M. Acosta, L.A. Schmitt, L.M. Luna, M.C. Scherrer, M. Brilz, K.G. Webber, M. Deluca, H.J. Kleebe, J. Rödel, W. Donner, Core–shell lead–free piezoelectric ceramics: current status and advanced characterization of the $Bi_{1/2}Na_{1/2}TiO_3$–$SrTiO_3$ system. J. Am. Ceram. Soc. **98**, 3405–3422 (2015)
22. H.L. Li, Q. Liu, J.J. Zhou, K. Wang, J.F. Li, H. Liu, J.Z. Fang, Grain size dependent electrostrain in $Bi_{1/2}Na_{1/2}TiO_3$-$SrTiO_3$ incipient piezoceramics. J. Eur. Ceram. Soc. **36**, 2849–2853 (2016)
23. S.H. Kim, S.H. Lee, H.S. Han, J.S. Lee, Piezoelectric characteristics of lead-free $0.74(Bi_{0.5}Na_{0.5})TiO_3$–$0.26SrTiO_3$ ceramics according to calcination temperature. J. Korean Inst. Electr. Electron. Mater. Eng. **32**, 35–39 (2019)
24. T.A. Duong, H.S. Han, Y.H. Hong, Y.S. Park, H.T.K. Nguyen, T.H. Dinh, J.S. Lee, Dielectric and piezoelectric properties of $Bi_{1/2}Na_{1/2}TiO_3$–$SrTiO_3$ lead–free ceramics. J. Electroceram. **41**, 73–79 (2018)
25. Y. Watanabe, Y. Hiruma, H. Nagata, T. Takenaka, Phase transition temperatures and electrical properties of divalent ions (Ca^{2+}, Sr^{2+} and Ba^{2+}) substituted $(Bi_{1/2}Na_{1/2})TiO_3$ ceramics. Ceram. Int. **34**, 761–764 (2008)
26. W. Bai, L. Li, W. Wang, B. Shen, J. Zhai, Phase diagram and electrostrictive effect in BNT-based ceramics. Solid State Commun. **206**, 22–25 (2015)
27. Y. Gong, X. He, C. Chen, Z. Yi, Large electric field-induced strain in ternary $Bi_{0.5}Na_{0.5}TiO_3$–$BaTiO_3$–Sr_2MnSbO_6 lead-free ceramics. Ceram. Int. **45**, 7173–7179 (2019)
28. Y.H. Hong, H.S. Han, G.H. Jeong, Y.S. Park, T.H. Dinh, C.W. Ahn, J.S. Lee, High electromechanical strain properties by the existence of nonergodicity in $LiNbO_3$–modified $Bi_{1/2}Na_{1/2}TiO_3$–$SrTiO_3$ relaxor ceramics. Ceram. Int. **44**, 21138–21144 (2018)
29. A. Ullah, M. Alam, A. Ullah, C.W. Ahn, J.S. Lee, S. Cho, I.W. Kim, High strain response in ternary $Bi_{0.5}Na_{0.5}TiO_3$–$BaTiO_3$–$Bi(Mn_{0.5}Ti_{0.5})O_3$ solid solutions. RSC Adv. **6**, 63915–63921 (2016)
30. J. Hao, W. Li, J. Zhai, H. Chen, Progress in high-strain perovskite piezoelectric ceramics. Mater. Sci. Eng. R Rep. **135**, 1–57 (2019)
31. T. Zheng, J. Wu, D. Xiao, J. Zhu, Recent development in lead-free perovskite piezoelectric bulk materials. Prog. Mater. Sci. **98**, 552–624 (2018)
32. W. Krauss, D. Schütz, F.A. Mautner, A. Feteira, K. Reichmann, Piezoelectric properties and phase transition temperatures of the solid solution of $(1–x)(Bi_{0.5}Na_{0.5})TiO_{3-x}TiO_3$. J. Eur. Ceram. Soc. **30**, 1827–1832 (2010)
33. J. Koruza, V. Rojas, L.M. Luna, U. Kunz, M. Duerrschnabel, H.J. Kleebe, M. Acosta, Formation of the core–shell microstructure in lead-free $Bi_{1/2}Na_{1/2}TiO_3$–$SrTiO_3$ piezoceramics and its influence on the electromechanical properties. J. Eur. Ceram. Soc. **36**, 1009–1016 (2016)
34. T. Frömling, S. Steiner, A. Ayrikyan, D. Bremecker, M. Dürrschnabel, L.M. Luna, H.J. Kleebe, H. Hutter, K.G. Webber, M. Acosta, Designing properties of $(Na_{1/2}Bi_x)TiO_3$-based materials

through A-site non-stoichiometry. J. Mater. Chem. C **6**, 738–744 (2018)
35. E. Aksel, J.L. Jones, Phase formation of sodium bismuth titanate perovskite during solid-state processing. J. Am. Ceram. Soc. **93**, 3012–3016 (2010)
36. H. Tagawa, K. Kimura, T. Fujino, K. Ouchi, Reactivity of starting materials in formation of strontium titanate. Denki Kagaku **52**, 154–159 (1984)
37. H.S. Han, W. Jo, J. Rödel, I.K. Hong, W.P. Tai, J.S. Lee, Coexistence of ergodicity and nonergodicity in $LaFeO_3$-modified $Bi_{1/2}(Na_{0.78}K_{0.22})_{1/2}TiO_3$ relaxors. J. Phys. Condens. Matter **24**, 365901 (2012)
38. K. Wang, A. Hussain, W. Jo, J. Rödel, D.D. Viehland, Temperature-dependent properties of $(Bi_{1/2}Na_{1/2})TiO_3$-$(Bi_{1/2}K_{1/2})TiO_3$-$SrTiO_3$ lead-free piezoceramics. J. Am. Ceram. Soc. **95**, 2241–2247 (2012)
39. W. Jo, S. Schaab, E. Sapper, L.A. Schmitt, H.J. Kleebe, A.J. Bell, J. Rödel, On the phase identity and its thermal evolution of lead free $(Bi_{1/2}Na_{1/2})TiO_3$-6 mol% $BaTiO_3$. J. Appl. Phys. **110**, 074106 (2011)
40. H.S. Han, W. Jo, J.K. Kang, C.W. Ahn, I.W. Kim, K.K. Ahn, J.S. Lee, Incipient piezoelectrics and electrostriction behavior in Sn-Doped $Bi_{1/2}(Na_{0.82}K_{0.18})_{1/2}TiO_3$ lead-free ceramics. J. Appl. Phys. **113**, 154102 (2013)
41. T.H. Dinh, J.K. Kang, J.S. Lee, N.H. Khansur, J. Daniels, H.Y. Lee, F.Z. Yao, K. Wang, J.F. Li, H.S. Han, W. Jo, Nanoscale ferroelectric/relaxor composites: origin of large strain in lead–free Bi–based incipient piezoelectric ceramics. J. Eur. Ceram. Soc. **36**, 3401–3407 (2016)
42. N. Chen, W. Yao, C. Liang, S. Xiao, J. Hao, Z. Xu, R. Chu, Phase structure, ferroelectric properties, and electric field-induced large strain in lead-free $0.99[(1-x)(Bi_{0.5}Na_{0.5})TiO_{3-x}(Bi_{0.5}K_{0.5})TiO_3]$–0.01Ta piezoelectric ceramics. Ceram. Int. **42**, 9660–9666 (2016)
43. V.D.N. Tran, A. Ullah, T.H. Dinh, J.S. Lee, Large field-induced strain properties of $Sr(K_{0.25}Nb_{0.75})O_3$-modified $Bi_{1/2}(Na_{0.82}K_{0.18})_{1/2}TiO_3$ lead-free piezoelectric ceramics. J. Electron. Mater. **45**, 2627–2631 (2016)
44. M. Chandrasekhar, P. Kumar, Synthesis and characterizations of $SrTiO_3$ modified BNT-KNN ceramics for energy storage applications. J. Electroceram. **38**, 111–118 (2017)
45. A. Hussain, C.W. Ahn, J.S. Lee, A. Ullah, I.W. Kim, Large electric-field-induced strain in Zr-modified lead-free $Bi_{0.5}(Na_{0.78}K_{0.22})_{0.5}TiO_3$ piezoelectric ceramics. Sens. Actuator A-Phys. **158**, 84–89 (2010)
46. C.W. Ahn, C.H. Hong, B.Y. Choi, H.P. Kim, H.S. Han, Y. Hwang, W. Jo, K. Wang, J.F. Li, J.S. Lee, A brief review on relaxor ferroelectrics and selected issues in lead-free relaxors. J. Korean Phys. Soc. **68**, 1481–1494 (2016)
47. M. Tachibana, E.T. Muromachi, Thermal conductivity and heat capacity of the relaxor ferroelectric $[PbMg_{1/3}Nb_{2/3}O_3]_{1-x}[PbTiO_3]_x$. Phys. Rev. B. **79**, 100104(R) (2009)
48. N. Novak, R. Pirc, M. Wencka, Z. Kutnjak, High-resolution calorimetric study of $Pb(Mg_{1/3}Nb_{2/3})O_3$ single crystal. Phys. Rev. Lett. **109**, 037601 (2012)
49. A. Zaman, A. Hussain, R.A. Malik, A. Maqbool, S. Nahm, M.H. Kim, Dielectric and electromechanical properties of $LiNbO_3$-modified $(BiNa)TiO_3$–$(BaCa)TiO_3$ lead-free piezoceramics. J. Phys. D Appl. Phys. **49**, 175301 (2016)
50. K.N. Pham, A. Hussain, C.W. Ahn, W. Kim, S.J. Jeong, J.S. Lee, Giant strain in Nb-doped $Bi_{0.5}(Na_{0.82}K_{0.18})_{0.5}TiO_3$ lead-free electromechanical ceramics. Mater. Lett. **64**, 2219–2222 (2010)
51. S.T. Zhang, A.B. Kounga, E. Aulbach, T. Granzow, W. Jo, H.J. Kleebe, J. Rödel, Lead-free piezoceramics with giant strain in the system $Bi_{0.5}Na_{0.5}TiO_3$–$BaTiO_3$–$K_{0.5}Na_{0.5}NbO_3$. I. Structure and room temperature properties. J. Appl. Phys. **103**, 034107 (2008)
52. D.S. Lee, D.H. Lim, M.S. Kim, K.H. Kim, S.J. Jeong, Electric field-induced deformation behavior in mixed $Bi_{0.5}Na_{0.5}TiO_3$ and $Bi_{0.5}(Na_{0.75}K_{0.25})_{0.5}TiO_3$-$BiAlO_3$. Appl. Phys. Lett. **99**, 062906 (2011)
53. T.H. Dinh, J.K. Kang, H.T.K. Nguyen, T.A. Duong, J.S. Lee, V.D.N. Tran, K.N. Pham, Giant strain in lead-free relaxor/ferroelectric piezocomposite ceramics. J. Korean Phys. Soc. **68**, 1439–1444 (2016)
54. A. Khaliq, M. Sheeraz, A. Ullah, J.S. Lee, C.W. Ahn, I.W. Kim, Large strain in $Bi_{0.5}(Na_{0.78}K_{0.22})_{0.5}TiO_3$–$Bi(Mg_{0.5}Ti_{0.5})O_3$ based composite ceramics under low driving field. Sens. Actuator A Phys. **258**, 174–181 (2017)